Pyridine-based lanthanide complexes: towards bimodal agents operating as near infrared luminescent and MRI reporters†

Laurent Pellegatti,[ab] Jian Zhang,[c] Bohuslav Drahos,[a] Sandrine Villette,[a] Franck Suzenet,[b] Gérald Guillaumet,[b] Stéphane Petoud*[ac] and Éva Tóth*[a]

Received (in Cambridge, UK) 2nd October 2008, Accepted 23rd October 2008
First published as an Advance Article on the web 12th November 2008
DOI: 10.1039/b817343e

We report two prototype Ln^{3+} complexes that address requirements for both MRI and luminescence imaging and we demonstrate that the presence of two H_2O molecules bound to the Ln^{3+}, beneficial for MRI applications of the Gd^{3+} analogue, is not a major limitation for the development of NIR luminescent agents.

Among the state-of-the-art bioimaging modalities, some are characterized by high resolution but low sensitivity (magnetic resonance imaging, MRI), others by high sensitivity but low resolution (optical imaging). Luminescent/MRI bimodal imaging offers the advantage of coupling the high sensitivity of luminescence with the high resolution of MRI.[1] Lanthanide complexes are well suited for the design of bimodal imaging probes: they combine optimized magnetic and optical properties, while the similar chemical reactivities allow facile substitution of one Ln^{3+} by another. Gd^{3+} complexes are efficient MRI contrast agents.[2,3] Several Ln^{3+} cations emit in the visible[4] or in the near infrared (NIR).[5] NIR imaging is more compatible with biological applications: (i) the lack of native NIR fluorescence in biological systems makes the detection highly sensitive, (ii) the low scattering of NIR photons allows for a better image resolution,[6] (iii) NIR photons can cross significant tissue depths for non-invasive imaging.[7] In addition, lanthanides provide complementary properties over organic fluorophores: resistance to photobleaching, long luminescence lifetimes, no reabsorption, sharp emission bands.[4,5] So far, the development of lanthanide chelators combining MRI and luminescence activities has been modest.[8–12] The combined requirements for both imaging techniques were considered to be non-compatible: the inner sphere H_2O required for MRI is expected to induce dramatic quenching of the Ln^{3+} luminescence through non-radiative deactivation.[13] Evidently, bimodal probes have to account for the differences in sensitivity of the imaging modality. An MRI reporter (Gd^{3+} complex) has to be administered in at least $\sim$100 fold higher concentration than the luminescent optical probe. Being aware of this, bimodal agents are still attractive as they enable the colocalization of the acquired images providing a powerful way to validate *in vivo* experiments.[1] The majority of bimodal agents reported so far are Gd^{3+} complexes or iron-oxide nanoparticles conjugated to fluorescent organic dyes.[1]

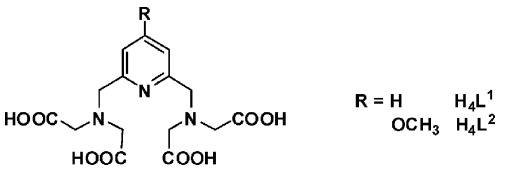

Scheme 1 Structure of the ligands L^1 and L^2.

We report prototypes of a versatile scaffold for Ln^{3+} complexation where MRI and luminescence requirements are both satisfied using the same ligand. Through the appropriate choice of a pyridine-based backbone, L^1 and L^2 ensure (i) high MRI efficacy when complexed to Gd^{3+}, due to bishydration of the chelate, (ii) efficient sensitization of a NIR emitting Ln^{3+} when complexed to Nd^{3+} (Scheme 1). They also fulfil the requirements of thermodynamic stability and kinetic inertness, prerequisite for biological applications of metal complexes. We demonstrate for the first time that the presence of two H_2O molecules bound to the Ln^{3+}, beneficial for MRI applications of the Gd^{3+} analogue, is not an absolute limitation for the development of NIR luminescent probes. This work opens promising routes towards Ln^{3+}-based bimodal contrast agents for MRI and NIR optical imaging. So far, only one bimodal MRI/luminescence agent with a NIR emitting Ln^{3+} has been described.[10] In that approach, the lanthanide sensitization was obtained through a Re complex and not an organic sensitizer. L^1 was previously proposed for the development of bimodal imaging probes, however, only visible luminescent Ln^{3+} cations were considered.[11,14]

The absorption spectrum of NdL^1 shows a unique absorption band (Fig. 1; for NdL^2 see ESI†). Upon excitation of the absorption band, the NIR emission spectra reveal three narrow emission bands that correspond to Nd^{3+} transitions (895, 1051 and 1323 nm assigned to transitions from the $^4F_{3/2}$ level to the $^4I_{9/2}$, $^4I_{11/2}$ and $^4I_{13/2}$ sublevels). These experiments demonstrate that the electronic structures of L^1 and L^2 can sensitize Nd^{3+}. Importantly, emission signals were observed with a good detection sensitivity using a commercial fluorimeter.

The luminescence lifetimes recorded upon ligand excitation in H_2O and D_2O allow the presence of two H_2O coordinated to Ln^{3+} in EuL^1 and EuL^2 to be concluded (Table 1).[13] The quantum yields, characterizing the efficiency of the sensitization and protection of lanthanide cations by L^1 and L^2, are

[a] *Centre de Biophysique Moléculaire, CNRS, rue Charles Sadron, 45071 Orléans, France. E-mail: eva.jakabtoth@cnrs-orleans.fr; Fax: +33 2 38 63 15 17; Tel: +33 2 38 25 76 25*
[b] *Institut de Chimie Organique et Analytique, UMR 6005 CNRS/ Université d'Orléans, Rue de Chartres, 45067 Orléans, France*
[c] *Dept. of Chemistry, The University of Pittsburgh, 219 Parkman Avenue, 15260 Pittsburgh, USA. E-mail: spetoud@pitt.edu*
† Electronic supplementary information (ESI) available: Synthesis of the ligands, details of luminescence, potentiometric and kinetic measurements. See DOI: 10.1039/b817343e

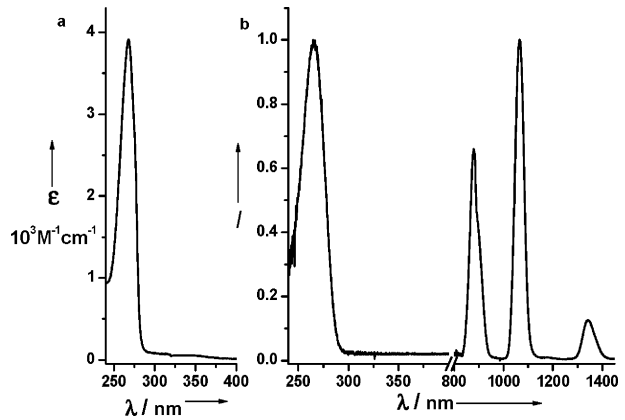

Fig. 1 Absorption (a), normalized emission (λ_{ex} = 267 nm) and excitation (λ_{em} = 1065 nm) spectra (b) of 5.1×10^{-4} M NdL^1. 0.01 M HEPES, pH 7.02, I = 0.01 M.

Table 1 Luminescence quantum yields and lifetimes of Nd^{3+} and Eu^{3+} complexes of L^1 and L^2 (10^{-4} M, 0.01 M HEPES, I = 0.01 M, pH = 7.02)

		L^1	L^2
Nd^{3+}	Φ_{H_2O}	$9.7(4) \times 10^{-5a}$	$7.5(7) \times 10^{-5b}$
	τ_{H_2O} (μs)[c]	0.059(1)	0.072(1)
	Φ_{D_2O}	$5.5(2) \times 10^{-4a}$	$4.0(3) \times 10^{-4b}$
	τ_{D_2O} (μs)[c]	0.310(1)	0.314(2)
Eu^{3+}	τ_{H_2O} (ms)[c]	0.403(1)	0.35(4)
	τ_{D_2O} (ms)[c]	1.85(2)	1.79(6)
	q	2.1	2.4

[a] λ_{ex} = 266 nm. [b] λ_{ex} = 250 nm. [c] λ_{ex} = 266 nm.

remarkable for a bishydrated Nd^{3+} complex. They are in the same range as those of the non-hydrated Nd-T2soxMe (0.027%), a system optimized for fully protecting the NIR emitting Ln^{3+} for aqueous application.[15] This result demonstrates for the first time that the non-radiative deactivation of NIR emitting lanthanides, even resulting from two water molecules, can be compensated by an efficient ligand to lanthanide energy transfer.

Ternary complex formation with endogenous donors can be an important limitation to the MRI use of bishydrated Gd^{3+} chelates. The relaxivity of GdL^1, r_1 = 6.21 mM^{-1} s^{-1} (25 °C, 500 MHz), remains unaffected in bovine serum, indicating that the inner sphere H_2O molecules are not replaced by potential donor groups. The emission spectra of EuL^1 recorded in pure water and in the presence of 600 equivalents of carbonate or phosphate (pH 7.4) are identical, excluding the formation of ternary complex.

The toxicity of Ln^{3+} complexes depends on the release of free Ln^{3+}, controlled by the thermodynamic stability and kinetic inertness. Zn^{2+} and Cu^{2+} were found to be particularly active in transmetallation of acyclic Ln^{3+} chelates.[16] Stability constants determined by pH-potentiometry demonstrate a significant selectivity of L^1 and L^2 for Gd^{3+} *vs.* Ca^{2+}, Zn^{2+} and Cu^{2+} (Table 2). It has been also shown that the formation of the dinuclear Zn_2DTPA (H_5DTPA = diethylenetriamine-pentaacetic acid) is an important driving force in the transmetallation of GdDTPA.[16] Such a dinuclear complex is not detectable with L^1 and L^2, which can likely be explained by their rigidity. No transmetallation of $LnL^{1,2}$ is observed in the presence of a 100-fold excess of

Table 2 Complex stability constants and pM values[ab]

	L^1		L^2	DTPA[d]
log K_{GdL}	18.60 ± 0.02	18.1[c]	18.76 ± 0.01	22.46
log K_{NdL}	18.76 ± 0.01	—	18.28 ± 0.01	—
log K_{ZnL}	15.84 ± 0.02	15.3[c]	16.93 ± 0.01	18.29
log K_{ZnHL}	3.81 ± 0.02	—	3.70 ± 0.01	5.6
log K_{ZnH2L}	—	—	—	3.1
log K_{Zn2L}	—	—	—	4.48
log K_{CuL}	15.69 ± 0.02		15.53 ± 0.02	21.5
log K_{CuHL}	3.45 ± 0.02	—	3.37 ± 0.02	4.8
log K_{CaL}	9.43 ± 0.06	9.2[c]	9.81 ± 0.01	10.1
pGd[e]	17.5[f]	—	17.6[f]	19.1[f]
pGd[e]	9.8[g]	—	9.9[g]	11.2[g]

[a] K_{ML} = [ML]/[M][L]; K_{MHL} = [MHL]/[ML][H^+]. [b] The protonation constants, log K_{Hi}, are 8.95, 7.85, 3.38, 2.48 and 8.91, 7.85, 3.01, 2.42 for L^1 and L^2, respectively. [c] Ref. 18. [d] Ref. 19. [e] pGd = −log $[Gd]_{free}$. [f] $c_{Gd} = 10^{-6}$ M, $c_L = 10^{-5}$ M, pH 7.4. [g] $c_{Gd} = 10^{-6}$ M, $c_L = 10^{-5}$ M, $c_{Zn} = 10^{-5}$ M, pH 7.4.

Zn^{2+} or Cu^{2+}, in contrast to GdDTPA under identical conditions.[16] The rigid pyridinic skeleton also contributes to the slowness of the acid-catalyzed dissociation. We studied the proton catalyzed dissociation of GdL^1 in the exchange reaction $GdL^1 + Eu^{3+} \rightarrow EuL^1 + Gd^{3+}$, under pseudo-first order conditions (pH 3.6–5.2; c_{GdL} = 0.5 mM, c_{Eu} = 5–30 mM). The observed rate constants show a quadratic dependency on [H^+] ($k_{obs} = k_0 + k_1[H^+] + k_2[H^+]^2$). The constants characterizing the dissociation *via* mono- and diprotonated complexes are $k_1 = 0.17 \pm 0.08$ M^{-1} s^{-1} and $k_2 = 520 \pm 30$ M^{-2} s^{-1}, lower values than those for GdDTPA, k_1 = 0.58 M^{-1} s^{-1} and $k_2 = 9.7 \times 10^4$ M^{-2} s^{-1}.[16] Since the dissociation pathway *via* Zn^{2+} or Cu^{2+} transmetallation, which represents 98% of the overall dissociation for GdDTPA under physiological conditions,[16] is not important for GdL^1, and the proton catalyzed dissociation is also slower, GdL^1 has a remarkable inertness for a bishydrated chelate.

At this proof of principle stage of the project, we demonstrated that even bishydrated Nd^{3+} complexes can have a quantum yield in the same range as those of the most optimized chelates so far reported. The LnL^1 chelates are remarkably inert, and do not form ternary complexes, in contrast to DO3A-type chelates.[17] These properties make the pyridinic synthon a prime candidate for the development of bimodal MRI/NIR imaging probes. In the perspective of biological applications, we are modifying the ligand structure by attaching different substituents to the pyridine to shift the excitation wavelength towards higher values in order to prevent damages to biological samples and to allow deeper tissue penetration of the excitation photons. These structural modifications, however, will not influence the bishydrated nature and kinetic inertness of the complexes. The pyridine-based platform provides high synthetic versatility. It offers easy routes for coupling the probes to biological vectors and to increase the molecular size in order to optimize proton relaxivity.

This work was financially supported by the Institut National du Cancer, La Ligue contre le Cancer, France, the National Science Foundation (award DBI0352346) and was carried out in the frame of the COST Action D38. S.P. gratefully acknowledges Le Studium (Agency for research and international hosting associate researchers in "Region Centre"), Orléans, France, for financial support.

Notes and references

1 (*a*) L. Frullano and T. Meade, *J. Biol. Inorg. Chem.*, 2007, **12**, 939; (*b*) W. J. M. Mulder, G. J. Strijkers, R. Koole, C. D. M. Donega, G. Storm, A. W. Griffioen and K. Nicolay, *Bimodal Liposomes and Paramagnetic QD-Micelles for Multimodality Molecular Imaging of Tumor Angiogenesis in Nanoparticles in Biomedical Imaging*, Springer, New York, 2007.

2 P. Caravan, J. J. Ellison, T. J. McMurry and R. B. Lauffer, *Chem. Rev.*, 1999, **99**, 2293.

3 *The Chemistry of Contrast Agents in Medical Magnetic Resonance Imaging*, ed. A. E. Merbach and É. Tóth, Wiley, Chichester, 2001.

4 (*a*) S. Petoud, S. M. Cohen, J.-C. G. Bünzli and K. N. Raymond, *J. Am. Chem. Soc.*, 2003, **125**, 13324; (*b*) J.-C. G. Bünzli and C. Piguet, *Chem. Soc. Rev.*, 2005, **34**, 1048.

5 J. Zhang, P. D. Badger, S. J. Geib and S. Petoud, *Angew. Chem., Int. Ed.*, 2005, **44**, 2508.

6 J. V. Frangioni, *Curr. Opin. Chem. Biol.*, 2003, **7**, 626.

7 R. Weissleder, *Nat. Biotechnol.*, 2001, **19**, 316.

8 I. Nasso, C. Galaup, F. Havas, P. Tisnès, C. Picard, S. Laurent, L. Vander Elst and R. N. Muller, *Inorg. Chem.*, 2005, **44**, 8293.

9 S. G. Crich, L. Biancone, V. Cantaluppi, D. Duo, G. Esposito, S. Russo, G. Camussi and S. Aime, *Magn. Reson. Med.*, 2004, **51**, 938.

10 T. Koullourou, L. S. Natrajan, H. Bhavsar, S. J. A. Pope, J. Feng, J. Narvainen, R. Shaw, E. Scales, R. Kauppinen, A. M. Kenwright and S. Faulkner, *J. Am. Chem. Soc.*, 2008, **130**, 2178.

11 S. Laurent, L. Vander Elst, M. Wautier, C. Galaup, R. N. Muller and C. Picard, *Bioorg. Med. Chem. Lett.*, 2007, **17**, 6230.

12 R. J. Aarons, J. K. Notta, M. M. Meloni, J. Feng, R. Vidyasagar, J. Narvainen, S. Allan, N. Spencer, R. A. Kauppinen, J. S. Snaith and S. Faulkner, *Chem. Commun.*, 2006, 909.

13 A. Beeby, I. M. Clarkson, R. S. Dickins, S. Faulkner, D. Parker, L. Royle, A. S. de Sousa, J. A. G. Williams and M. Woods, *J. Chem. Soc., Perkin Trans. 2*, 1999, 493.

14 C. Gunanathan, A. Pais, E. Furman-Haran, D. Seger, E. Eyal, S. Mukhopadhyay, Y. Ben-David, G. Leitus, H. Cohen, A. Vilan, H. Degani and D. Milstein, *Bioconjugate Chem.*, 2007, **18**, 1361.

15 S. Comby, D. Imbert, C. Vandevyver and J.-C. G. Bünzli, *Chem.–Eur. J.*, 2007, **13**, 936.

16 L. Sarka, L. Burai and E. Brücher, *Chem.–Eur. J.*, 2000, **6**, 719.

17 S. Aime, M. Botta, J. I. Bruce, V. Mainero, D. Parker and E. Terreno, *Chem. Commun.*, 2001, 115.

18 S. Jakab, Z. Kovacs, L. Burai and E. Brücher, *Magy. Kém. Foly.*, 1993, **99**, 391.

19 L. D. Pettit and K. J. Powell, *IUPAC Stability Constants Database*, version 4.11, Academic Software, Yorks, UK, 1999.